David O. Hearshen, PhD • James H. Ellis, MD • Paul L. Carson, PhD
• Paul Shreve, BS • Alex M. Aisen, MD

Boundary Effects from Opposed Magnetization Artifact in IR Images[1]

A cancellation of signal intensity at the interface separating selected tissue-equivalent materials is observed in inversion recovery proton MR images. The absence of signal intensity at the interface is always one pixel wide and appears only when the tissue-equivalent materials forming the interface differ substantially in their longitudinal relaxation times (T1). Images were obtained of various two-layer combinations of tissue-equivalent materials consisting of vegetable oil, animal fat, saline, aqueous Mn^{+2}, or 2% agar doped with Mn^{+2}. This type of boundary is compared with chemical shift artifacts, which at 0.15 T and 0.35 T produce a similar effect. A clinical example of the opposed magnetization artifact is also shown. Since tissues with substantially different T1s are found in vivo, it is expected that this effect could lead to an instrument-dependent artifact that could easily be misinterpreted.

Index terms: Magnetic resonance (MR), chemical shift • Magnetic resonance, physics

Radiology 1986; 160:543–547

As THE number of techniques for magnetic resonance (MR) imaging grow and improvements in signal-to-noise ratios (S/N) and resolution are made, radiologists are confronted with a large number of image acquisition and display options. By selecting a suitable technique, radiologists can enhance the contrast between normal and abnormal tissues in a region of interest. Variation of timing parameters in standard pulse sequences (partial saturation [PS], spin echo [SE], and inversion recovery [IR]) can selectively enhance the desired region. Clinicians have great interest in selectively using timing parameters to distinguish tumor from edema or to distinguish malignant tumors from benign ones. Ideally, clinicians would like to delineate the boundaries of tumors exactly in order to measure their size and extent.

Using various approximations, a number of authors have modeled pulse sequences and predicted the effect of these sequences on image contrast with various standard instrument settings (i.e., repetition time [TR], echo delay [TE], and inversion time [TI]) (1–6). In addition, proton density, which previously had been thought not to be a factor in image contrast, has been shown to influence the appearance of brain images, especially when the effects of the other parameters tend to cancel each other (1, 5, 6).

In this paper, we show that the IR pulse sequence reveals an instrument setting-dependent artifact that appears as a thin, dark line, always one pixel wide. We term this effect the "opposed magnetization artifact." The origin of the boundary is similar but not identical to the "bounce point" artifact reported elsewhere (4). This artifact is also not the same as the chemical shift artifact that can be found on both SE and IR images (7). The nature of and differences between these two artifacts will be discussed.

After observing the opposed magnetization artifact while looking for other effects, we offered a hypothesis (8) and tested it on boundaries between materials with widely different T1s. We determined the effect could occur between materials with smaller differences in T1 and could be demonstrated in a clinical image. Thus, the effect will occur between numerous tissues in certain IR images.

Boundary Artifacts in IR Images

The equation modeling the time evolution of the magnetization in an IR sequence was derived previously (9):

$$M_z(\mathrm{TI}, \mathrm{TR}) = M_0(1 - 2e^{-\mathrm{TI}/\mathrm{T1}} + e^{-\mathrm{TR}/\mathrm{T1}}), \quad (1)$$

where M_z is the longitudinal magnetization and M_0 is the magnetization equilibrium.

Because many methods of MR image reconstruction display the absolute value of the Fourier transform, the time dependence of the magnetization, which is proportional to the signal strength, has the appearance shown in Figure 1. For a tissue with a given T1, the absolute value M_z decreases to a null value then increases to its equilibrium value. The time at which M_z has its minimum value has been called the "bounce" or "null" point (4). The relative value of M_z at a given time is a function of a physical characteristic of the tissue, T1, and machine settings (TR and TI). Many machines, including the three used for these experiments, add an additional 180° pulse to the IR pulse sequence to produce a spin echo (SE) (i.e., an IR-SE sequence). This additional pulse adds a T2 effect, which to first order can be modeled as (1)

[1] From the Department of Diagnostic Radiology, Henry Ford Hospital, 2799 W. Grand Blvd., Detroit, MI 48202 (D.O.H.) and the Department of Radiology, University of Michigan, Ann Arbor (J.H.E., P.L.C., P.S., A.M.A.).
Received April 2, 1985; revision requested May 20, 1985; final revision accepted April 23, 1986. Supported in part by Public Health Service grant Rol CA 31857 awarded by the National Cancer Institute and by grant PDT 242 from the National Cancer Society. **Address reprint requests to** D.O.H.

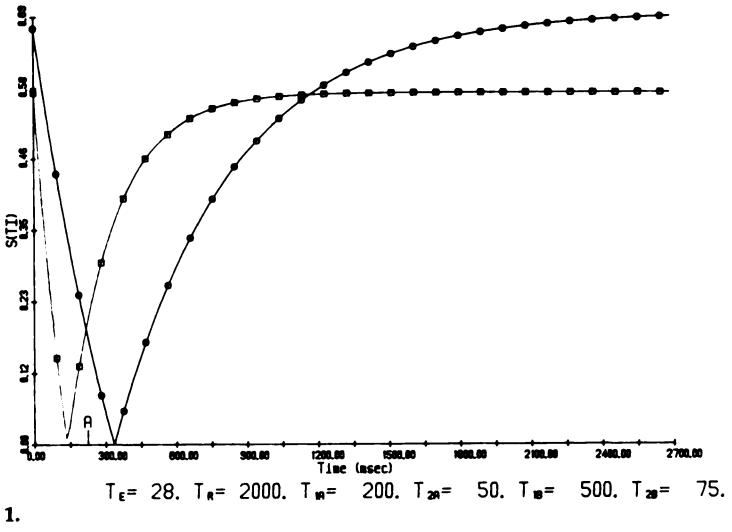

1.

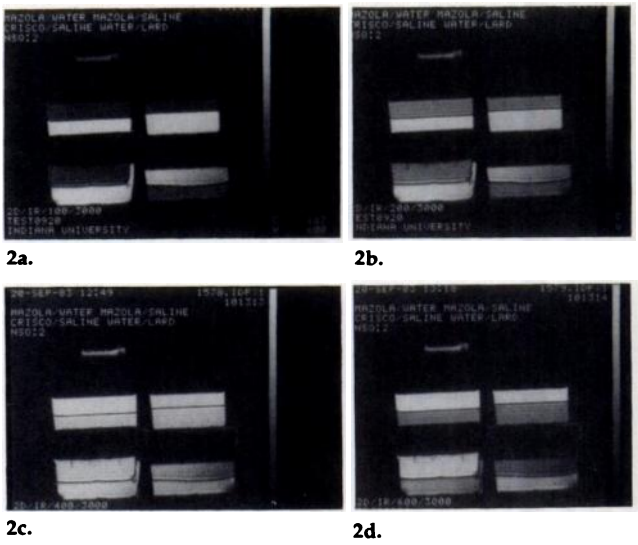

2a. 2b. 2c. 2d.

Figures 1, 2. Absolute value of the signal (proportional to the longitudinal magnetization) versus TI in an IR-SE sequence for materials having different T1s. The bounce points are where the curves intersect the x-axis. At the TI labeled *A* (approximately 275 msec), the magnetization of one material is equal in magnitude but opposite in direction to the other. **(2)** IR-SE images of four two-layer combinations. Clockwise, from upper left of each photo, the top/bottom materials are: mazola/water, mazola/saline, water/lard, Crisco/saline. TR = 3 sec for all images **(a)** TI = 100 msec. **(b)** TI = 200 msec. **(c)** TI = 400 msec. **(d)** TI = 600 msec. Note the change in relative intensity of the two layers with TI. This and all subsequent images have a resolution of 1.7 mm unless stated otherwise.

$$S(\mathrm{TI}, \mathrm{TR}) = M_0(1 - 2e^{-\mathrm{TI}/\mathrm{T1}} + e^{-\mathrm{TR}/\mathrm{T1}})e^{-\mathrm{TE}/\mathrm{T2}}, \quad (2)$$

where S is the signal amplitude detected at TE seconds after t = TI. For a given TE, the effect is just to multiply the curve by a constant factor, exp(−TE/T2) (Fig. 1). We have neglected second order corrections in TE and T2 that may become important for small TR (10). If we solve equation (2) for S equal to zero, we get the value of TI for the null point; however, the estimate of TI = (0.69) (T1) for the null point (4) can be highly inaccurate if TR is not large compared to T1. A more correct expression is

$$\mathrm{TI} = -\mathrm{T1} \ln\left(\frac{1 + e^{-\mathrm{TR}/\mathrm{T1}}}{2}\right) \quad (3)$$

For instance, if TR = 1 second and T1 = 500 msec, equation (3) gives 283 msec, while TI = (0.69) (T1) gives 346 msec, a 22% error.

When two different materials are considered, the situation can be described using Figure 1. If the two materials have different T1s and T2s, their respective bounce points can occur at different times. Several authors pointed out that the contrast between two contiguous tissues can be increased if TI is chosen at or near the bounce point of one of them (1, 4).

Another effect, the opposed magnetization artifact, can occur if TI is chosen not at the bounce point of one of the materials but at a point where the longitudinal magnetization of each material is approximately equal in magnitude but opposite in direction relative to the external field B_0. This corresponds to point *A* in Figure 1, where the negative slope part of one curve intersects the positive slope part of the other curve. With this TI, the signals emitted from the two materials will be 180° out of phase and will destructively interfere such that the net signal is small only in the pixels in which both materials are found, namely, along the boundary separating them. Those pixels that consist entirely of one material or the other will appear with equal intensity. The net effect will be to have two materials appearing relatively bright but separated by a thin, dark line. Since only those pixels that span the physical boundary show destructive interference, the size of the boundary is defined by the pixel dimensions (resolution).

Chemical Shift Artifacts

The chemical shift of protons in lipids relative to water produces well-documented effects in imaging, especially at higher fields (7, 11–13). The effect of the chemical shift is a displacement in the frequency encoding direction. The size of this spatial shift is on the order of typical resolution values and results in computer-generated misregistration of fat-containing signals by a pixel or two relative to the spatial locations of the water signals. This produces a signal void where the fat has shifted away from the water and an increase in signal where the fat has shifted into the water-containing pixels. The signal void, which is approximately one pixel wide, may have a similar appearance to the opposed magnetization artifact.

MATERIALS AND METHODS

Two different imaging systems were used to detect and explain these artifacts: a whole-body Technicare (Cleveland, Ohio) 0.15-T resistive system at Indiana University and a 0.35-T Diasonics (Milpitas, Calif.) superconductive system at the University of Michigan. The main features of these machines have been described elsewhere (14, 15). An additional experiment was performed on a 1.5-T General Electric Signa system at Henry Ford Hospital. The ability to modify TI and TE on this system allowed us to visualize the opposed magnetization artifact at different TIs.

Various materials were used in these experiments, including mineral and vegetable oils, lard, saline, and tap water. Aqueous Mn^{+2} and Mn^{+2}-doped agar were also used to generate nonfat-containing materials with relatively short T1s. Immiscible materials were placed in large plastic test tubes or open plastic containers. Cellophane was used as a physical barrier when diffusion of Mn^{+2} between materials was evident. In one case, liquids were injected into sealed containers that were then immersed in a tub of tap water.

RESULTS

Figure 2 shows the boundary effect on a 0.15-T IR-SE image between water

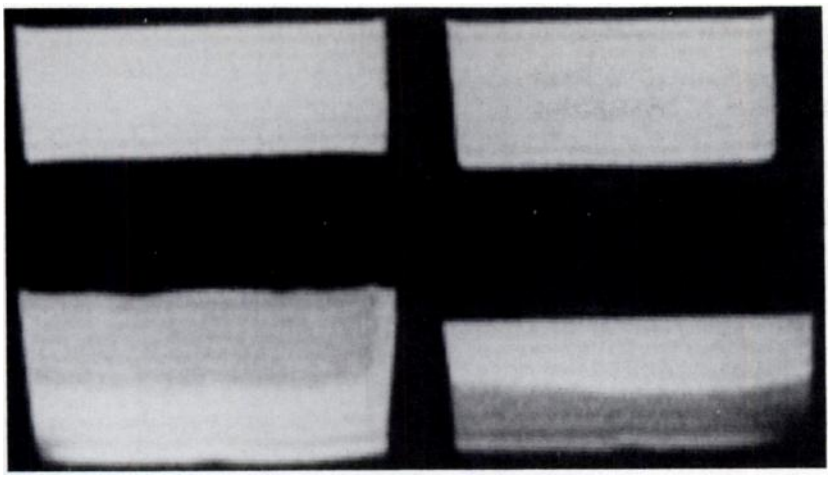

3.

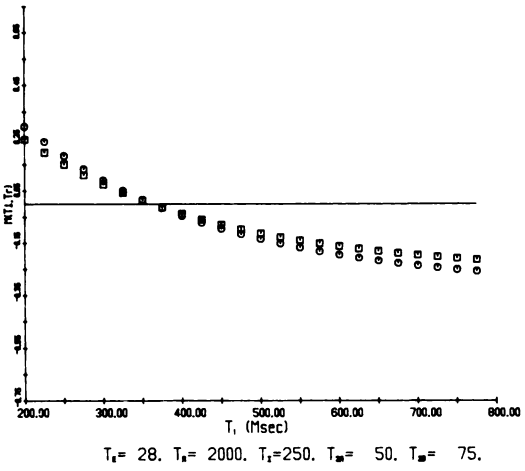

4.

Figures 3, 4. SE 2,500/60 (TR msec/TE msec) images at 0.15 T of the same materials as in Figure 2. The contrast between the material is approximately the same as that in the IR-SE images in Figure 2c, but no boundary exists. The Crisco and the lard are darker on the T2-weighted image and demonstrate relatively short T2s. **(4)** Computer simulation of the longitudinal magnetization for fixed TE, TR, and TI as a function of T1 for two different T2s. A boundary exists for two materials having T1s such that the distance below the centerline (zero magnetization) for one is equal to the distance above the line for the other. Squares represent T2 = 50 msec; circles represent T2 = 75 msec.

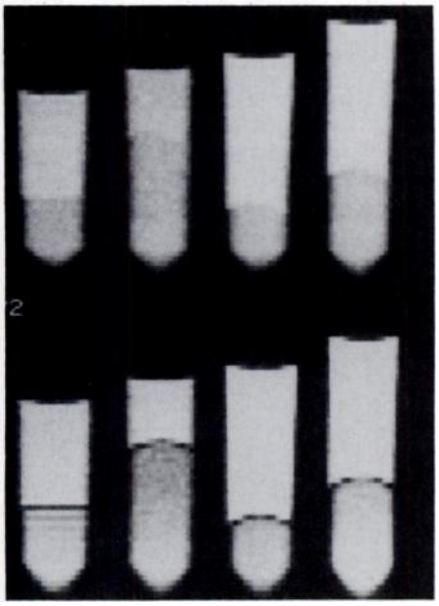

Figure 5. IR-SE 1,900/210/28 (TR msec/TI msec/TE msec) (lower) and SE 2,000/28 image (upper) at 0.35 T. From left to right in both rows: vegetable oil/agar, vegetable oil/aqueous Mn^{+2}, mineral oil/tap water, mineral oil/tap water. The boundary is independent of resolution and field strength. The graying of the boundary is a partial volume effect.

or saline and oil or other fatlike materials. The boundary is clearly visible when one layer has a long T1 (saline, >2 secs) and the other has a short T1 (oil, <200 msec). Figure 2 shows the effect of varying TI for the same set of materials. The boundary is enhanced at a TI of 400 msec, though it is still visible at TI = 200 and 600, where the relative intensities of the layers are not equal. This is because all four tubs contain material with a very long T1 (water or saline) and material with a very short T1 (oil or fat). For water or saline with a T1 greater than 2 seconds, the lower bound (using T1 = .69 TI) for the null point is 1.7 seconds. For oil with a T1 of about 200 msec, the null point occurs at about 140 msec. At TIs of 200, 400, and 600 msec, the longitudinal magnetization of the oil phase is positive and the longitudinal magnetization of the water phase is still negative, resulting in some cancellation. The effect in images with TIs of 100 msec is more ambiguous. For the two tubs containing oil (top left and top right, Fig. 2a), 100 msecs is shorter than the null points of both the oil and water. In this situation, the longitudinal magnetizations of both oil and water are negative. No cancellation occurs, and no boundary is seen. In the two bottom tubs of Figure 2a, more solid materials, Crisco on the left and lard on the right, were used. These solid materials should have a shorter T1 than oil, and the much more solid lard should have a shorter T1 than the softer Crisco. If the T1 of these materials is less than about 150 msec, their longitudinal magnetizations will have become positive at 100 msec, resulting in a cancellation with the longitudinal magnetization of water in the boundary pixels. The boundary is clearly seen in the water/lard container and is ambiguous in the Crisco/saline container. While T1 measurements from these images may not be accurate, the numbers we calculated using the manufacturer's software are consistent with this explanation. At 0.15 T they are: oil, 175 msec; Crisco, 147 msec; and lard, 137 msec.

Even though the boundary effect varies for the materials and the TIs shown in Figure 1, all the images have an appearance distinctly different from the SE image shown in Figure 3. With the same spatial resolution and approximately the same contrast, no boundary is observed in the SE image.

To examine the dependence of the opposed magnetization artifact on T1 and T2, we simulated the relative intensities for a number of T1-T2 combinations at a specific TR, TE and TI. A typical result is shown in Figure 4. The object was to pick materials and machine settings that maximized the relative intensities while maintaining a clearly visible boundary. Though our study is not exhaustive, a general trend is that the conditions that favor visualization of the boundary are long TR, short TE, and a two-layer combination of materials with a T1 less than 300 msec coupled with materials that have a T1 greater than 500 msec. TI is not a continuous variable on the UM machine, so graphs like the one in Figure 4 are necessary to estimate the T1s of pairs of materials that will demonstrate the boundary effect. From Figure 1 it is apparent that a boundary will exist only for TI between the null points of the two materials. We have neglected differences in proton density between the two materials in these simulations. Small differences in proton density will effect visualization of the boundary (see Discussion).

Materials with different T1 combinations were imaged at 0.15 T and 0.35 T. For a given instrument setting, only a small range of T1 combinations will give a boundary. Figure 5 shows some combinations with Mn^{+2}-doped agar, aqueous Mn^{+2}, or tap water as the bottom phase and vegetable or mineral oil as the top phase. As in Figure 3, the SE images show no boundary for various combinations of materials even though the contrast is similar to that in the IR-SE images. The boundary is continuous for the flat oil/agar interface on the

left. For the other three tubes with liquids in both phases, the curved nature of the physical boundary produces additional partial volume effects (graying of the boundary) where the physical boundary cuts across the edge of a pixel.

Figure 6 shows the T2 effect on the boundary condition. Since the bottom phase (water) has a longer T2, the relative intensities are more nearly equal on the second echo, thus enhancing the boundary. In an IR-SE sequence, the opposed magnetization artifact is a function of T1, T2, and the respective machine parameters TI and TE, consistent with equation (2).

An example of the opposed magnetization artifact seen in high-field imaging is shown in Figure 7. T1 and T2 were measured for both oil (top phase) and tap water (bottom phase) using the manufacturer's software. A total of eight different points (TE = 25, 40, 50, 75, 80, 100, 120, and 160 msec) were used for the T2 calculation, and six points (TR = 300, 500, 800, 1,000, 2,500, and 4,000 msec) were used for the T1 calculation. The results of the calculation gave 328 msec and 50 msec for the T1 and T2 of the oil and 4,530 msec and 900 msec for the T1 and T2 of the water at 1.5 T. The only difference between the images in Figure 7a and 7b is the TI. In Figure 7a (TI = 370 msec), the boundary is clearly demonstrated near the calculated crossover point (analogous to point *A* in Fig. 1). In Figure 7b, no boundary is evident at a TI of 1,200 msec, where the signals from both materials have the same phase. This figure not only shows the field independence of the opposed magnetization artifact but also shows that flexibility in the control of the pulse sequence parameters allows the double-valued nature of IR magnitude reconstruction to be demonstrated. The materials are isointense in both images with different imaging parameters, but the boundary only appears in Figure 7a, in which the signals from the two materials are 180° out of phase.

The difference between chemical shift artifacts and phase cancellation boundaries is shown in Figures 8 and 9. In these experiments, a thin plastic container was filled with either mineral oil or an aqueous $MnCl_2$ solution. At 0.35 T, both materials had T1s of approximately 200 msec. The thickness of the walls of the container (<0.1 mm) was much smaller than the resolution (1.7 mm). Both containers were immersed in water and imaged simultaneously. On the SE image, the chemical shift artifact is shown to be only in the frequency encoding direction (horizontal). The black band on the right of the oil container is where the oil signal has shifted away from the water, leaving a signal void. The bright rim on the left is where the oil signal overlaps the water signal. There is no edge effect in the vertical, phase-encoding direction. No edge effect is seen on the $MnCl_2$ container.

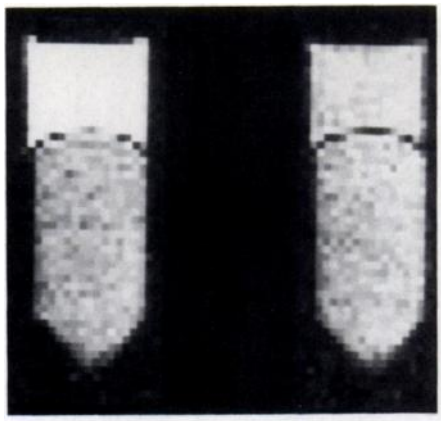

Figure 6. IR-SE image at 0.35 T of oil/water interface. Left is the first echo (TE = 28 msec) and right is the second echo (TE = 56 msec). Note the longer T2 of water gives an enhanced boundary on the second echo where the intensities are more nearly equal, but a boundary does exist for unequal intensities on the first echo.

In the IR-SE image, both containers exhibit the boundary effect in every pixel that contains the boundary between the container and the surrounding water. In addition, the oil container also exhibits the chemical shift artifact.

The opposed magnetization artifact is demonstrated in an image of a healthy volunteer in Figure 10. With the pulse sequence parameters listed in the figure, the magnetization from the white matter is near the null point but is recovered past zero. The more slowly relaxing magnetizations of the gray matter and CSF are still negative, resulting in the boundary between both white matter and gray matter and between white matter and CSF.

DISCUSSION

Both of the artifacts discussed have been seen in clinical images. The chemical shift artifact is more pronounced at higher fields, but it is important to note its appearance at lower fields (0.35–0.6 T) in order not to mistake the artifact edge for an anatomic structure (such as a blood vessel). One way to test for the effect, as demonstrated earlier, is to look for a difference in the edge between pixels that separate fat and water in the phase-encoding and frequency-encoding directions. These three different effects—flow void from small vessels, chemical shift artifacts, and opposed magnetization artifacts—can all have a similar appearance on any one image. It is important to distinguish these effects in IR-SE images in order to avoid diagnostic errors.

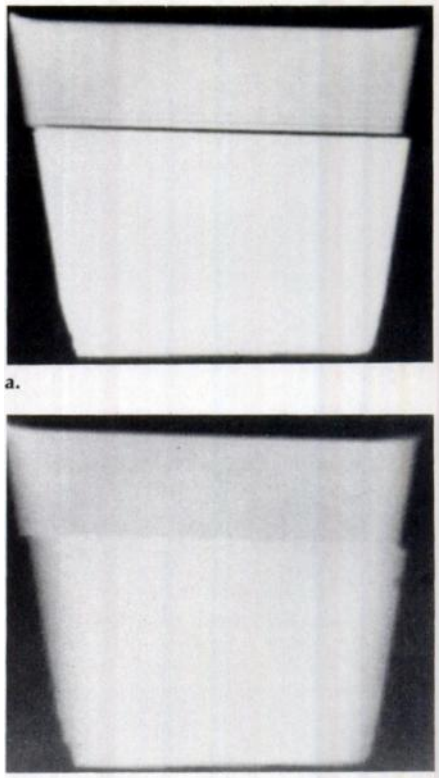

a.

b.

Figure 7. IR-SE image at 1.5 T of oil/water interface. **(a)** 2,000/370/50 image. **(b)** 2,000/1,200/50 image. The resolution in both images is 0.625 mm. The relative signal intensities of the oil and water are the same in the two images, but the boundary only exists in the image with the shorter TI in which the signals from the materials are 180° out of phase.

The opposed magnetization artifact in IR or IR-SE images depends not on the relative chemical shift between two phases but on the difference in their T1 values. The requirement for a signal-free boundary is not, as the computer simulations suggest, that TI be exactly at that time where the magnetization per unit volume of one material is equal in magnitude but opposite in direction to the other, but that it falls between the null points of the two materials. Figure 9 shows a well-defined boundary even though the intensities of the two materials are unequal. This is a consequence of the pixel size being much larger than the physical boundary. If the magnetizations per unit volume of the two materials are unequal and opposite in direction, the opposed magnetization artifact will occur in those pixels with a proportionately larger volume of the material with the lower signal strength. Partial volume effects (graying of the boundary) do occur when the physical boundary just cuts across the corner of a pixel, as in Figures 5 and 6.

The appearance of the opposed magnetization artifact is a consequence of

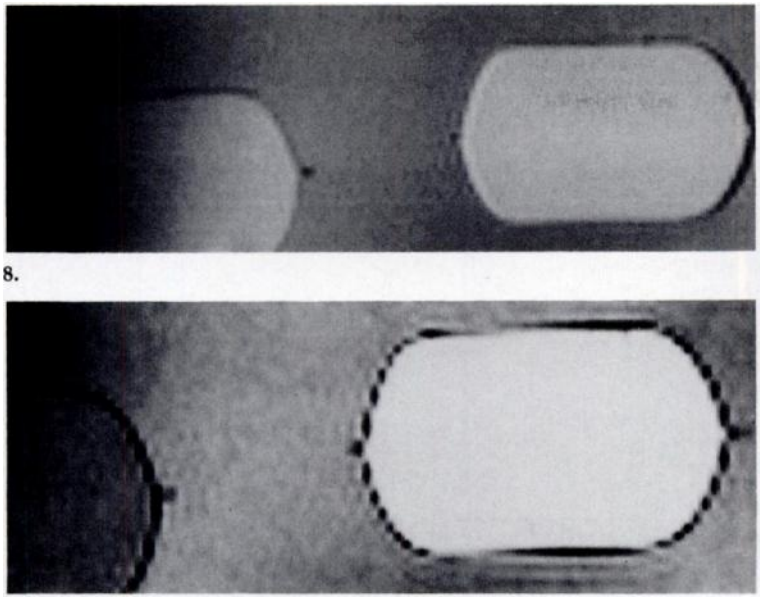

8.

9.

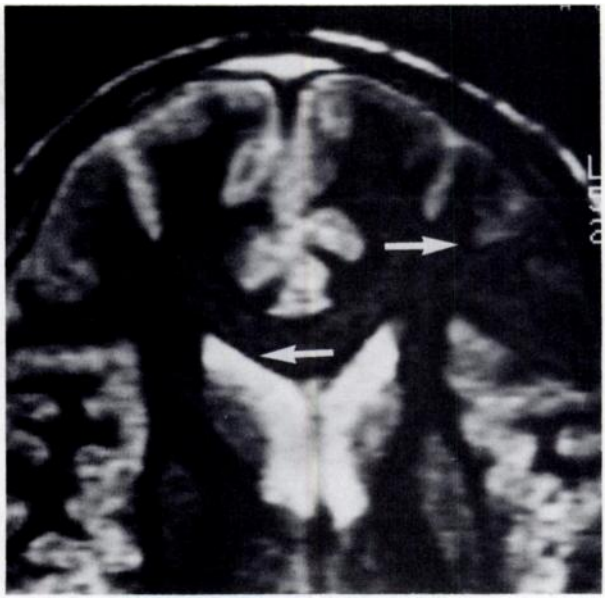

10.

Figures 8-10. SE image at 0.35 T of two plastic containers immersed in water. The container on the left is filled with aqueous $MnCl_2$. The container on the right is filled with oil; the chemical shift is clearly seen on this container in the frequency encoding direction as a bright band on the left and a dark band on the right. **(9)** IR-SE image at 0.35 T with the same materials as Figure 8. Here the boundary effect can be seen encircling both containers in both phase encoding and frequency encoding directions. The thickness of the walls of the containers (<0.1 mm) is much smaller than the resolution (1.7 mm). The T1 of both the oil and the $MnCl_2$ solution is approximately 200 msec. **(10)** Magnified transverse IR-SE 1,500/300/25 image of the head at 1.5 T. The section thickness was 5 mm, the field of view for the nonmagnified image was 24 cm, and the matrix size 128 × 256. The boundary exists between both cerebrospinal fluid (CSF) and white matter (left arrow) and between gray and white matter (right arrow).

the reconstruction technique; reconstruction that retains phase information would result in a different mapping of the signals from tissues with short and long T1s. Cancellation would still occur, but the interface would appear as a gray border between a bright region (short T1) and a dark region (long T1).

The opposed magnetization artifact (Fig. 10) is harder to distinguish from flow-void effects than the chemical shift artifact. Comparison of IR-SE and SE images of the same region, however, will show no boundary in the SE image. This kind of artifact may be used to define the border between two areas in a region of interest, particularly if one tissue has a long T1. Since use of this effect requires knowledge of T1s, it may not be practical on a routine basis; however, improvements in S/N and resolution may make it useful as a specialty sequence for delineating exactly the boundary of a desired region. For example, a small malignant growth on the wall of a breast cyst surrounded by fat might be visible as a break in the opposed magnetization border, even though the lesion might be smaller than a pixel. With use of this method, small irregularities in the border of a lesion might prove to be a sensitive indicator of malignancy, particularly in regions such as the mediastinum or in the breasts of older women. The smoothness of the border between cartilage and synovial fluid could also be studied in this manner. Infiltration of one material into another could result in a region of pixels satisfying the boundary condition instead of a border one pixel wide. Using synthesized images, it might be possible to extrapolate to a different TI, obviating the need to know the T1s beforehand. ■

Acknowledgment: The authors thank Drs. Charles Meyer and Thomas Chenevert for their insightful suggestions.

References

1. Wehrli FW, MacFall JR, Shutts D, Breger R. Mechanisms of contrast in NMR imaging. J Comput Assist Tomogr 1984; 8:369-380.
2. Young IR, Burl M, Clark CJ, et al. Magnetic resonance properties of hydrogen: imaging the posterior fossa. AJR 1981; 137:895-901.
3. Crooks LE, Mills CM, Davis PL, et al. Visualization of cerebral and vascular abnormalities by NMR imaging: the effect of imaging parameters on contrast. Radiology 1983; 144:843-852.
4. Bradley WR. Effect of relaxation times on magnetic resonance image interpretation. Noninvasive Med Imaging 1984; 1:193-204.
5. Droege RT, Wiener SN, Rzeszotarski SB. A strategy for magnetic resonance imaging of the head: results of a semi-empirical model. Radiology 1984; 153:419-434.
6. Ortendahl DA, Hylton N, Kaufman L, et al. Analytical tools for magnetic resonance imaging. Radiology 1984; 153:479-488.
7. Cho ZH, Nalcioglu O, Park HW, Ra JB, Hilal SK. Chemical shift artifact correction scheme using echo-time encoding technique. Magn Reson Med 1985; 2:253-261.
8. Hearshen DO, Ellis JH, Carson PL, Aisen AM, Shreve P. Boundary effects from phase cancellation in inversion recovery images. Presented at the 3d Annual Meeting of the Society of Magnetic Resonance in Medicine, New York, August, 1984.
9. Dixon RL, Ekstrand K. The physics of proton NMR. Med Phys 1982; 9:807-818.
10. Lin MS. Measurement of spin lattice relaxation times in double spin echo imaging. Magn Reson Med 1984; 1:361-369.
11. Maudsley A, Hilal SK, Rerman WH, Simon HE. Spatially resolved high resolution spectroscopy by four dimensional NMR. J Magn Reson 1983; 51:147-152.
12. Mareci TH, Brooker HR. High resolution magnetic resonance spectra from a sensitive region defined by pulsed field gradients. J Magn Reson 1984; 57:157-163.
13. Babcock EE, Brateman L, Weinreb JC. Edge artifacts in MR images: a chemical shift effect. J Comput Assist Tomogr 1985; 9:252-257.
14. Ellis JH, Bies JR, Kopecky KK, Klatte EC, Rowland RG, Donahue JP. Comparison of NMR and CT imaging in the evaluation of metastatic retroperitoneal lymphadenopathy from testicular carcinoma. J Comput Assist Tomogr 1984; 8:709-719.
15. Crooks LE, Arakawa M, Hoenninger JC, et al. Nuclear magnetic resonance whole-body imager operating at 3.5 KGauss. Radiology 1982; 143:169-174.